ACS Macro Letters

Letter

pubs.acs.org/macroletters

Isoindigo-Based Donor−Acceptor Conjugated Polymers for Air-Stable Nonvolatile Memory Devices

Walaa Elsawy,[†,‡,∥] Myungwoo Son,[†,∥] Jisu Jang,[†] Myung Jin Kim,[†] Yongsung Ji,[†] Tae-Wook Kim,[§] Heung Cho Ko,[†] Ahmed Elbarbary,[‡] Moon-Ho Ham,*[,†] and Jae-Suk Lee*[,†]

[†]Center for Emerging Electronic Devices and Systems, Research Institute for Solar and Sustainable Energies (RISE), Department of Nanobio Materials and Electronics, School of Materials Science and Engineering, Gwangju Institute of Science & Technology, 123 Cheomdangwagi-ro, Buk-gu, Gwangju 500-712, Republic of Korea

[‡]Department of Chemistry, Faculty of Science, Tanta University, Tanta 31527, Egypt

[§]Soft Innovative Materials Research Center, Institute of Advanced Composite Materials, Korea Institute of Science and Technology, Wanjusandan 6-ro, Bongdong-eup, Wanju-gun, Joellabuk-do 585-905, Republic of Korea

Supporting Information

ABSTRACT: Nonvolatile resistive memory devices based on a new low bandgap donor−acceptor (D−A) conjugated polymer, poly((*E*)-6,6′-bis(2,3-dihydrothieno[3,4-*b*][1,4]dioxine-5-yl)-1,1′-bis(2-octyldodecyl)-[3,3′-biindolinyi-dene]-2,2′-dione) (PIDED), which are fabricated and operated in ambient air, are reported. The D−A conjugated polymer is synthesized from 2,3-dihydrothieno[3,4-*b*][1,4]dioxine and isoindigo as an electron donor and an electron acceptor, respectively, using CH-arylation polymerization. The devices show nonvolatile, unipolar resistive switching behaviors with a high on/off current ratio (~10^4), excellent endurance cycles (>200 cycles), and a long retention time (>10^4 s) in ambient air. These properties remain stable in ambient air over one year, demonstrating that the device performance is significantly unaffected by exposure to air as the isoindigo has strong electron-withdrawing character and the PIDED exhibits a high degree of crystallinity. This study may pave the way for use of practical nonvolatile organic memory devices operating in ambient air.

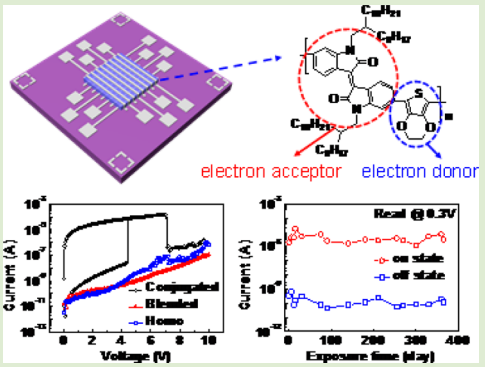

Organic memories are currently being investigated as promising candidates for information storage media due to easy fabrication processing, low cost, flexibility, scalability, and printability, which could be advantageous for future applications in flexible devices.[1,2] Various polymers such as polythiophene, polyvinylcarbazole, and polyimide have been used as polyelectrolytes or matrices in doped or mixed systems.[3] To improve memory effects, many research groups have incorporated inorganic nanoparticles[4] or carbon nanomaterials (e.g., carbon nanotube,[5] graphene,[6,7] or fullerene[8]) into polymer matrices, which could influence both switching characteristics (write-once-read-many times,[7] unipolar,[8] and bipolar switching[4,5]) and memory performance.[5,6] However, the uniform dispersion of nanoscale particles in a polymer is difficult to achieve because of agglomeration, which could worsen memory performance.[9] Consequently, the design of polymers containing both electron-donor and electron-acceptor moieties within a repeating unit remains an active area of research for organic memory applications.

Donor−acceptor (D−A) copolymers could provide the electronic transition between ground and excited states that is required for use as active layers in memory devices. Furthermore, they effectively avoid the ion aggregation problem and, consequently, allow for a uniform film morphology that leads to excellent device performance.[10,11] In D−A conjugated polymer systems, the charge transfer between donor and acceptor moieties can be controlled by the strength and ordering of donor and acceptor materials, as these parameters play a critical role in enhancing electrically bistable switching behavior.[12] Chen et al. synthesized D−A conjugated polymers consisting of selenophene and 3,6-dithiophen-2-yl-2,5-dialkylpyrrolo[3,4-*c*]pyrrole-1,4-dione that showed transistor-type nonvolatile memory properties.[13] Isoindigo has strong electron-withdrawing character due to its two lactam rings, making it useful as an acceptor moiety in D−A conjugated polymers.[14] Moreover, the planar π-conjugated symmetric structure of isoindigo imparts high crystallinity and stability. These properties make it an ideal monomer for the synthesis of low-bandgap D−A polymeric materials for electronic applications. Nevertheless, while several research groups have studied organic photovoltaic devices using isoindigo-based D−A polymeric materials as photoactive layers,[14,15] its memory effects have not yet been investigated. Additionally, although some polymer systems that exhibited memory effects in ambient air have been reported,[16] there have been relatively

Received: November 3, 2014
Accepted: February 26, 2015
Published: February 27, 2015

DOI: 10.1021/mz500698p
ACS Macro Lett. 2015, 4, 322−326

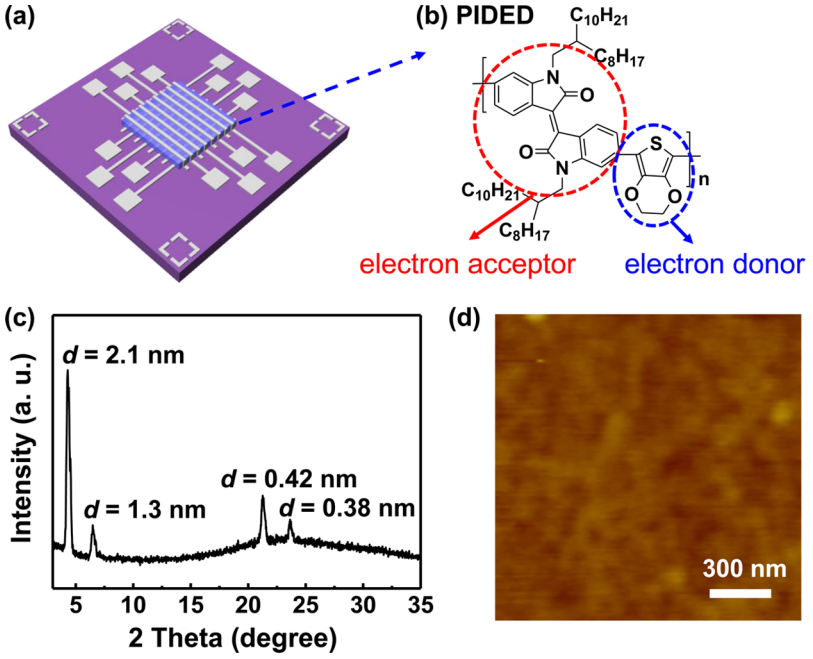

Figure 1. (a) Schematic of 8 × 8 crossbar array-type organic memory devices consisting of Al/polymer/Al. PIDED, PEDOT/PID blends, and PID homopolymer were used as active layers. (b) Structure of the conjugated polymer, PIDED, consisting of PEDOT and PID as the electron donor and acceptor moieties, respectively. (c) XRD spectrum and (d) AFM image of a conjugated polymer, PIDED film.

Scheme 1. Schematic Illustration of the Synthetic Route of Polymers: (a) PIDED and (b) PID

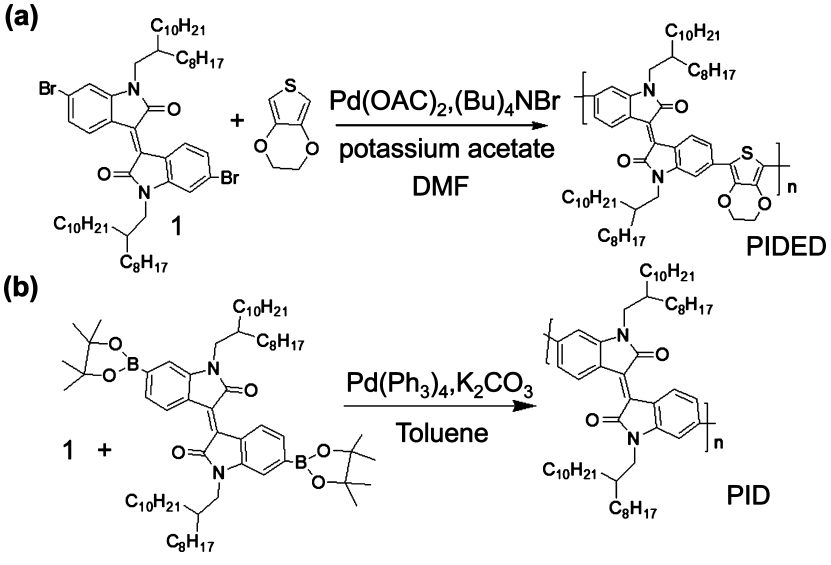

few examples of polymers with long-term environmental stability,[1,5,17] which should be overcome for practical applications.

In this study, we demonstrate air-stable nonvolatile resistive switching behaviors of metal−insulator−metal (MIM)-type memory devices based on a new low bandgap D−A conjugated polymer, poly((*E*)-6,6′-bis(2,3-dihydrothieno[3,4-*b*][1,4]-dioxine-5-yl)-1,1′-bis(2-octyldodecyl)-[3,3′-biindolinyi-dene]-2,2′-dione) (PIDED). This D−A conjugated polymer, which serves as an active layer in the device, was synthesized from 2,3-dihydrothieno[3,4-*b*][1,4]dioxine (EDOT) and isoindigo as an electron donor and an electron acceptor, respectively, using CH-arylation polymerization. The devices exhibited excellent air-stable memory performance with a high on/off current ratio (~10^4), excellent endurance cycles (>200 cycles), and a long retention time (>10^4 s), due to the low-lying HOMO levels of the isoindigo and a high degree of crystallinity of the PIDED.

Figure 1a shows a schematic of 8 × 8 crossbar array-type organic memory devices based on a polymeric layer sandwiched between two Al electrodes. To enable regular alternation of donor and acceptor moieties in polymeric films and to improve memory performance, the D−A conjugated polymer, PIDED, was synthesized as shown in Figure 1b and Scheme 1a. First, isoindigo was prepared from the condensation of bromoisatine with bromooxindole, followed by an alkylation reaction to produce the (*E*)-6,6′-dibromo-1,1-bis(2-octydodecyl)-(3,3′-biindolinylid-ene)-2,2′-dione (**1**) (Scheme 1). PIDED (M_n = 43.0 kDa) was then synthesized by CH-arylation polymerization[18] of compound **1** with EDOT in the presence of palladium acetate, potassium acetate, and tetrabutyl ammonium

DOI: 10.1021/mz500698p
ACS Macro Lett. 2015, 4, 322−326

bromide. For comparison, poly(*E*)-6-methyl-3-(6-methyl-1-(2-octyldodecyl)-2-oxoindolin-3-ylidene)-1-(2-octyldodecyl)-indolin-2-one (polyisoindigo (PID); M_n = 25.0 kDa) was synthesized by Suzuki cross-coupling of compound **1** with (*E*)-1,1′-bis(2-octyldodecyl)-6,6′-bis(4,4,5,5-tetramethyl-1,3,2-dioxaborolan-2-yl)-[3,3′-biindolinylidene]-2,2′-dione using Pd-$(Ph_3)_4$ (Scheme 1b). The polymers were purified by Soxhlet extraction with methanol, hexane, and acetone for 24 h each to remove catalyst residues. The polymers showed high solubility in common organic solvents. In this work, we prepared three different polymers (D−A conjugated (PIDED), D−A blended (poly(2,3-dihydrothieno[3,4-*b*][1,4]dioxin-5-yl) (PEDOT)/PID), and acceptor alone (PID) polymers). X-ray diffraction (XRD) patterns of the PIDED films confirmed that the as-coated PIDED was amorphous, while the annealed PIDED formed crystalline structure in the thin film due to $\pi-\pi$ intermolecular interactions (d values of 0.38 and 0.42 nm) and intermolecular packing via alkyl−alkyl interdigitations (d values of 1.3 and 2.1 nm) (Figure 1c and Figure S1, Supporting Information).[19−22] AFM measurements revealed that the PIDED had micrometer-sized rod-like structure with the width of ∼100 nm and the length of ∼1 μm (the root-mean-square (rms) roughness of 0.35 nm) due to intermolecular interactions, whereas the PID showed fibril-like structure (the rms roughness of 0.27 nm) (Figure 1d and Figure S2a, Supporting Information). These observations apparently support that the PIDED has the crystalline structure as confirmed by the XRD spectrum (Figure 1c). In contrast, the PEDOT/PID blends showed spherical agglomerates of the PEDOT in the PID matrix (the rms roughness of 2.3 nm) due to differences in the solubility of the two components (Figure S2b, Supporting Information). The donor polymers have poor solubility and become agglomerated in the acceptor polymer matrix, which has high solubility. Using these polymers, organic memory devices were fabricated in ambient air. The thickness of all the active layers used in this study was ∼40 nm.

Representative current−voltage ($I-V$) curves of the devices fabricated from the D−A conjugated polymer, PIDED, measured in ambient air are shown in Figure 2a. Each cell in the devices clearly exhibited typical unipolar resistive switching characteristics that occurred under the same bias polarity. When the applied voltage was swept from 0 to 5 V, the devices were switched from the initial high-resistance state (HRS, OFF state) to the low-resistance state (LRS, ON state) at a threshold voltage of approximately 4.5 V (i.e., the set or writing process). The devices displayed nonvolatile memory behavior, as they remained in the ON state during the voltage decrease, even after the applied voltage removal. In the second voltage sweep from 0 to 10 V, a sudden drop in current was observed when the applied voltage reached approximately 7 V, indicating the electrical transition from the LRS to the HRS (i.e., the reset or erasing process). For comparison, the as-coated PIDED was prepared and tested as a memory device. Although the as-coated PIDED has no crystalline nature (Figure S1, Supporting Information), the $I-V$ characteristics were similar to those of the annealed PIDED but had slightly lower on/off current ratio due to the lower on current (Figure S3, Supporting Information). To elucidate the switching stability and uniformity of the devices, the currents in the HRS and LRS for all cells in one device were measured at a read voltage of 0.3 V, and the cumulative probability distributions of the resistances in the HRS and LRS for all operative memory cells were plotted in Figure 2b. Although the distributions of

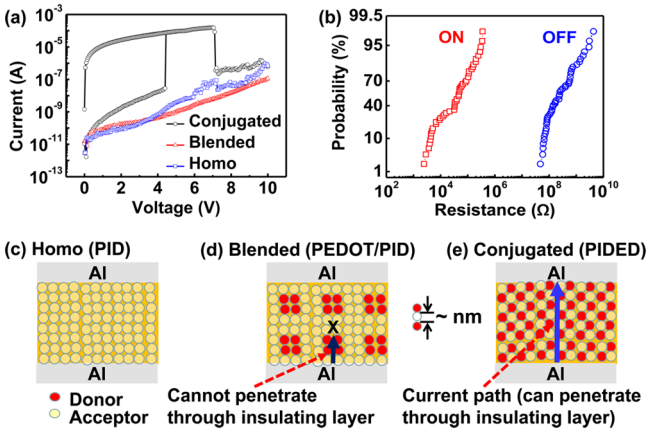

Figure 2. (a) $I-V$ curves of MIM-type memory devices fabricated from three different active polymers, measured in ambient air: D−A conjugated polymer, PIDED, D−A blended polymer, PEDOT/PID, and acceptor homopolymer, PID. (b) Cumulative probability characteristics of the switching current for all operative memory cells (48 operative cells out of 64 fabricated cells), measured at a read voltage of 0.3 V in ambient air. Schematics of current flow in three different polymer systems: (c) acceptor homopolymer, PID, (d) D−A blended polymer, PEDOT/PID, and (e) D−A conjugated polymer, PIDED.

the on- and off-resistance values are broad, it is important to note that the on and off resistances are separated by more than 1 order of magnitude. This difference is sufficient to distinguish each resistance state, indicating the good cell-to-cell uniformity of the device.

To investigate the effect of uniform dispersion of donor and acceptor groups in polymeric films on memory performance, we fabricated MIM-type devices from the D−A blended polymer (PEDOT/PID) and the acceptor homopolymer (PID) in addition to the PIDED. In contrast to the PIDED, the devices fabricated from the PEDOT/PID and the PID displayed low current levels with no resistive switching (Figure 2a), indicating that the charge transfer did not occur in these materials (Figures 2c and 2d, respectively). In the UV−vis−nIR absorption spectra, an absorption band from 500 to 900 nm was observed for the PIDED, which was lower than those of the PID and the PEDOT/PID (Figure S4a, Supporting Information). This redshift of the absorption band is attributed to strong intramolecular charge transfer and intermolecular $\pi-\pi$ stacking.[13] Thus, the alternation of strong donor and acceptor moieties in the conjugated PIDED polymer system can induce a low bandgap of 1.3 eV and a deep HOMO level at 4.9 eV. These properties, which were confirmed by UV−vis−nIR absorption and cyclic voltammetry measurements, impart conducting or semiconducting properties to the polymer (Figure S4, Supporting Information). Therefore, efficient charge transfer can occur along the polymer backbone. A conduction path can be generated in the polymeric layer by applying an external bias (Figure 2e). In addition, the strong dipole moments of the molecules help to sustain the conductive charge transfer state and thus result in nonvolatile behavior. To clarify the resistive switching mechanism, the $I-V$ curves of the PIDED device were plotted in a logarithmic scale (Figure S5, Supporting Information). The log I−log V curves can be divided into four regions with different slopes: $I \propto V$, $I \propto V^2$, $I \propto V^{3.4}$, and $I \propto V^2$. This is consistent with a space-charge-limited current (SCLC) model that consists of an Ohmic

DOI: 10.1021/mz500698p
ACS Macro Lett. 2015, 4, 322−326

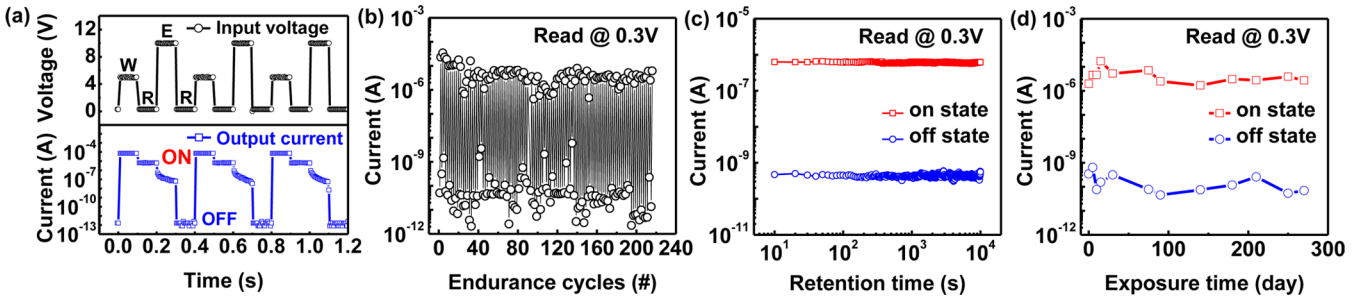

Figure 3. (a) WRER cycles of an Al/PIDED/Al memory device: the curves of the input voltage pulses (top) and the corresponding output current (bottom). (b) Endurance cycles and (c) retention time of an Al/PIDED/Al memory device. Two different current states (HRS and LRS) were read at 0.3 V after a writing voltage of 5 V and an erasing voltage of 10 V were alternately applied to the top electrode. (d) Evolution of the ON and OFF currents of an Al/PIDED/Al memory device as a function of exposure time to ambient air over a period of one year, obtained from *I*−*V* curves. The results indicate that the memory performance remains largely unaffected by the ambient air.

conduction region, a trap-limited SCLC region, a trap-filling region, and a trap-filled SCLC region.[6,23,24] Upon applying voltages, electrons are injected into the PIDED from the electrode and trapped by the acceptor moieties of the PIDED. At low voltages, the electrons do not have sufficient energy to escape from the acceptor moieties, and the current is low. At higher voltages, more electrons are injected into the PIDED, and the traps are nearly filled, which eventually causes the current to increase abruptly, reaching a SCLC. At further applied voltages, the traps are completely filled, and the device is switched to the ON state. Therefore, the bistable switching behavior can be explained by the trapped-charge-limited current mechanism.[6,23,24] In contrast, in the blended polymer system, the microphase separation of spherical structures takes place on the nanometer scale because of differences in the solubility of the components (Figure S2b, Supporting Information). This microphase-separated structure hinders efficient charge transfer between donors and acceptors, leading to high resistance and no resistive switching (Figure 2a).[15]

To further demonstrate their utility, we evaluated the reliability of the PIDED-based memory devices in terms of the write-read-erase-read (WRER) cycle, endurance, and retention measurements in ambient air (Figures 3a−3c, respectively). The switching cycle test was performed by applied repeated WRER cycles (5, 0.3, 10, and 0.3 V, respectively) in pulse mode. The pulse interval was 5 ms. After a write process at 5 V for 100 ms, the device was immediately switched to the ON state, followed by a read process at 0.3 V for 100 ms. After the write and read pulses, a voltage pulse of 10 V was applied to erase the device, which was detected by using a read voltage of 0.3 V. These results reveal that the switching time between the ON and OFF states is less than 5 ms.[25] Moreover, during more than 200 endurance cycles, both the ON and OFF states of the memory device were found to be stable with a high on/off ratio of approximately 4 orders of magnitude without any significant electrical degradation. These results confirm reproducible resistive switching. In addition, the memory device showed a stable retention time that exceeded 10^4 s.

Lastly, to confirm the environmental stability of the memory devices, which is a prerequisite for their use in practical devices, we exposed the memory device to ambient air and measured *I*−*V* curves over a period of one year (Figure S6, Supporting Information). The on and off currents obtained from the *I*−*V* curves were largely unaffected by exposure to the ambient air (Figure 3d). For comparison, memory devices were also measured in vacuum and nitrogen atmospheres (Figures S7 and S8, Supporting Information, respectively). The memory performances of both treatments were similar to that measured in ambient air, demonstrating that the environmental conditions do not significantly affect the memory performance of the PIDED-based memory devices. It might be attributed to the low-lying HOMO levels of the electron-deficient isoindigo.[26] Furthermore, the PIDED used in this work has a high degree of crystallinity (Figure 1c), which effectively prevents the diffusion of oxygen and water molecules to a crystalline polymer film from ambient air.[19]

In conclusion, we have demonstrated air-stable MIM-type memory devices based on PIDED with strong donor−acceptor moieties. Importantly, the PIDED-based memory devices were fabricated and operated in ambient air. They showed nonvolatile, unipolar resistive switching behaviors with a high on/off current ratio, excellent endurance cycles, and a long retention time in ambient air. These results were comparable to results obtained in vacuum and nitrogen atmospheres, demonstrating that device performance was unaffected by exposure to air. It is clear from the comparison of film morphology between the conjugated polymer, PIDED, and the blended polymer, PEDOT/PID, that the uniform dispersion of donor and acceptor groups in the polymeric film is responsible for intermolecular charge transfer and the memory performance. We believe that the design of conjugated polymers with the regular alternation of donor and acceptor moieties will enable the fabrication of practical organic memory devices operating in ambient air for versatile, high-performance, large-area electronics.

■ ASSOCIATED CONTENT

Supporting Information

Experimental details, XRD spectrum of an as-coated PIDED conjugated polymer, AFM images of PID and PEDOT/PID blended polymer, *I*−*V* curves of Al/PIDED/Al memory devices fabricated from as-coated and annealed PIDED films, UV−vis−nIR absorption spectra, cyclic voltammetry, and energy band diagram of polymers, log *I*−log *V* curves of an Al/PIDED/Al memory device, *I*−*V* curves of an Al/PIDED/Al memory device obtained over a period of one year in ambient air, memory characteristics of Al/PIDED/Al memory devices measured in vacuum and nitrogen atmospheres. This material is available free of charge via the Internet at http://pubs.acs.org.

DOI: 10.1021/mz500698p
ACS Macro Lett. 2015, 4, 322−326

AUTHOR INFORMATION

Corresponding Authors

*E-mail: mhham@gist.ac.kr (M.H.H.).
*E-mail: jslee@gist.ac.kr (J.S.L.).

Author Contributions

[‖]W.E. and M.S. contributed equally. The manuscript was written through contributions of all authors. All authors have given approval to the final version of the manuscript.

Notes

The authors declare no competing financial interest.

ACKNOWLEDGMENTS

This work was supported by Basic Science Research Program through the National Research Foundation of Korea (NRF) funded by the Ministry of Science, ICT & Future Planning (NRF-2013R1A1A1011215), Global Frontier Program through the Global Frontier Hybrid Interface Materials (GFHIM) of the National Research Foundation of Korea (NRF) funded by the Ministry of Science, ICT & Future Planning (2013M3A6B1078873), Research Institute for Solar and Sustainable Energies (RISE), and the GIST-Caltech Research Collaboration Project through a grant provided by GIST in 2014.

REFERENCES

(1) Hahm, S. G.; Kang, N. G.; Kwon, W.; Kim, K.; Ko, Y. G.; Ahn, S.; Kang, B. G.; Chang, T.; Lee, J. S.; Ree, M. *Adv. Mater.* **2012**, *24*, 1062−1066.
(2) Ji, Y.; Cho, B.; Song, S.; Kim, T. W.; Choe, M.; Kahng, Y. H.; Lee, T. *Adv. Mater.* **2010**, *22*, 3071−3075.
(3) Cho, B.; Song, S.; Ji, Y.; Kim, T. W.; Lee, T. *Adv. Funct. Mater.* **2011**, *21*, 2806−2829.
(4) Ouyang, J.; Chu, C. W.; Szmanda, C. R.; Ma, L.; Yang, Y. *Nat. Mater.* **2004**, *3*, 918−922.
(5) Hwang, S. K.; Lee, J. M.; Kim, S.; Park, J. S.; Park, H. I.; Ahn, C. W.; Lee, K. J.; Lee, T.; Kim, S. O. *Nano Lett.* **2012**, *12*, 2217−2221.
(6) Zhuang, X. D.; Chen, Y.; Liu, G.; Li, P. P.; Zhu, C. X.; Kang, E. T.; Neoh, K. G.; Zhu, J. H.; Li, Y. X. *Adv. Mater.* **2010**, *22*, 1731−1735.
(7) Zhuang, X. D.; Chen, Y.; Li, B. X.; Ma, D. G.; Zhang, B.; Li, Y. *Chem. Mater.* **2010**, *22*, 4455−4461.
(8) Song, S.; Cho, B.; Kim, T. W.; Ji, Y.; Jo, M.; Wang, G.; Choe, M.; Kahng, Y. H.; Hwang, H.; Lee, T. *Adv. Mater.* **2010**, *22*, 5048−5052.
(9) Zhong, G. L.; Kim, K.; Jin, J. I. *Synth. Met.* **2002**, *129*, 193−198.
(10) Zhuang, X. D.; Chen, Y.; Liu, G.; Zhang, B.; Neoh, K. G.; Kang, E. T.; Zhu, C. X.; Li, Y. X.; Niu, L. J. *Adv. Funct. Mater.* **2010**, *20*, 2916−2922.
(11) Kang, N. G.; Cho, B.; Kang, B. G.; Song, S.; Lee, T.; Lee, J. S. *Adv. Mater.* **2012**, *24*, 385−390.
(12) Wu, H. C.; Yu, A. D.; Lee, W. Y.; Liu, C. L.; Chen, W. C. *Chem. Commun.* **2012**, *48*, 9135−9137.
(13) Lin, H. W.; Lee, W. Y.; Chen, W. C. *J. Mater. Chem.* **2012**, *22*, 2120−2128.
(14) Zhang, G.; Fu, Y.; Xie, Z.; Zhang, Q. *Macromolecules* **2011**, *44*, 1414−1420.
(15) Wang, E.; Ma, Z.; Zhang, Z.; Henriksson, P.; Inganas, O.; Zhang, F.; Andersson, M. R. *Chem. Commun.* **2011**, *47*, 4908−4910.
(16) Lin, W. P.; Liu, S. J.; Gong, T.; Zhao, Q.; Huang, W. *Adv. Mater.* **2014**, *26*, 570−606.
(17) Qi, S.; Iida, H.; Liu, L.; Irle, S.; Hu, W.; Yashima, E. *Angew. Chem., Int. Ed.* **2013**, *52*, 1049−1053.
(18) Abdo, N. I.; El-Shehawy, A. A.; El-Barbary, A. A.; Lee, J. S. *Eur. J. Org. Chem.* **2012**, 5540−5551.
(19) Li, Y.; Singh, S. P.; Sonar, P. *Adv. Mater.* **2010**, *22*, 4862−4866.
(20) Avarvari, N.; Mezailles, N.; Ricard, L.; Floch, P. L.; Mathey, R. *Science* **1998**, *280*, 1587−1589.
(21) Lei, T.; Cao, Y.; Zhou, X.; Peng, Y.; Bian, J.; Pei, J. *Chem. Mater.* **2012**, *24*, 1762−1770.
(22) Kim, G.; Han, A. R.; Lee, H. R.; Lee, J.; Oh, J. H.; Yang, C. *Chem. Commun.* **2014**, *50*, 2180−2183.
(23) Bozano, L. D.; Kean, B. W.; Deline, V. R.; Salem, J. R.; Scott, J. C. *Appl. Phys. Lett.* **2004**, *84*, 607.
(24) Lin, H. T.; Pei, Z.; Chan, Y. J. *IEEE Electron Device Lett.* **2007**, *28*, 569−571.
(25) Kim, T. W.; Yang, Y.; Li, F.; Kwan, W. L. *NPG Asia Mater.* **2012**, *4*, e18.
(26) Zhuang, X. D.; Chen, Y.; Liu, G.; Li, P. P.; Zhu, C. X.; Kang, E. T.; Neoh, K. G.; Zhang, B.; Zhu, J. H.; Li, Y. X. *Adv. Mater.* **2010**, *22*, 1731−1735.

DOI: 10.1021/mz500698p
ACS Macro Lett. 2015, 4, 322−326